

UV-Assisted Graft Polymerization of Synthetic Membranes: Mechanistic Studies

Masahide Taniguchi,[†] John Pieracci,[†] William A. Samsonoff,[‡] and Georges Belfort*,[†]

Howard P. Isermann Department of Chemical Engineering, Rensselaer Polytechnic Institute, Troy, New York 12180-3590 and Wadsworth Center Laboratories, New York State Department of Health, Albany, New York 12201-0509

Received March 19, 2002. Revised Manuscript Received February 6, 2003

Mechanistic studies were conducted on UV-assisted graft polymerization of *N*-vinyl-2-pyrrolidinone (NVP) onto poly(ether sulfone) (PES) ultrafiltration (UF) membranes using a dip process. The molecular weight cutoff (MWCO) values of the UF membranes were 50, 70, and 100 kDa and the range of NVP monomer concentrations was 2–10 wt %. Our standard photooxidation protocol with 300-nm lamps was used. By operating below an irradiation energy, $E < 4 \text{ kJ/m}^2$, both homopolymerization and main-chain scission can be minimized with up to $C_{\text{NVP}} = 5 \text{ wt \%}$ NVP concentration for all three UF membranes. A universal linear plot of the net amount grafted versus monomer concentration times irradiation energy ($C_{\text{NVP}} \times E$) for $E < 4 \text{ kJ/m}^2$ was obtained for four NVP concentrations and three membranes. Resulting from graft polymerization, there appears to be a qualitative relationship between the thickness of the dense skin layer and the membrane surface roughness as measured by atomic force microscopy. Post-modification washing with ethanol was able to effectively remove entrapped homopolymer and other fragments. Also, UV-assisted graft polymerization of NVP on PES UF membranes effectively reduced irreversible membrane fouling. A protocol for optimizing graft-assisted photopolymerization of PES UF membranes is provided.

Introduction

Only a few polymers have been used to produce commercial synthetic membranes on a large scale because of the inordinate expense, long development lead-time, and relatively narrow requirements. Examples of those used include cellulosics, polyamides, polypropylenes, and polysulfones. However, many applications using membrane processes could benefit from the availability of a wider range of polymer chemistries and of more robust, lower fouling, and less expensive polymers.¹ Because companies are reticent to invest in the development of new polymers, alternate approaches such as the surface modification of widely used polymers (before casting) or of commercial membranes (post-casting) have been suggested. As a result, our group and others have utilized three main surface modification techniques: chemical,² photochemical,^{3,4} and low-temperature plasma.^{5–7} Of these, photochemical modifica-

tion has distinct advantages in simplicity, cost, and breadth of application. UV modification has been used widely for gas separation membranes,^{8–10} synthesis of pervaporation¹¹ and reverse osmosis membranes,^{12,13} and functionalization of ultrafiltration^{14–16} and environmentally (pH and temperature) sensitive^{17,18} membranes. Microfiltration^{19,20} membranes have been synthesized using photoinitiated cross-linking or monomer grafting. Much of the research conducted on the photomodification of ultrafiltration (UF) membranes has

* Corresponding author. E-mail: belfog@rpi.edu.

[†] Rensselaer Polytechnic Institute.

[‡] New York State Department of Health.

- (1) Strathmann, H. *AIChE J.* 2001, **47**, 1077–1087.
- (2) Nabe, A.; Staude, E.; Belfort, G. *J. Membr. Sci.* **1997**, *133*, 57–72.
- (3) Yamagishi, H.; Crivello, J. V.; Belfort, G. *J. Membr. Sci.* **1995**, *105*, 237–247.
- (4) Yamagishi, H.; Crivello, J. V.; Belfort, G. *J. Membr. Sci.* **1995**, *105*, 249–259.
- (5) Ulbricht, M.; Belfort, G. *J. Appl. Polym. Sci.* **1995**, *56*, 325–343.
- (6) Ulbricht, M.; Belfort, G. *J. Membr. Sci.* **1995**, *111*, 193–215.
- (7) Chen, H.; Belfort, G. *J. Appl. Polym. Sci.* **1999**, *13*, 1699–1711.

- (8) Kita, H.; Inada, T.; Tanaka, K.; Okamoto, K. *J. Membr. Sci.* **1994**, *87*, 139–147.
- (9) Matsui, S.; Ishiguro, T.; Higuchi, A.; Nakagawa, T. *J. Appl. Polym. Sci., Part B* **1997**, *35*, 2259–2269.
- (10) Matsui, S.; Ishiguro, T.; Higuchi, A.; Nakagawa, T. *J. Appl. Polym. Sci.* **1998**, *67*, 49–60.
- (11) Darkow, R.; Yoshikawa, M.; Kitao, T.; Tomaschewski, G.; Schellenberg, J. *J. Polym. Sci., Part A* **1994**, *32*, 1657–1664.
- (12) Chadda, S.; McCarry, B.; Childs, R.; Rogerson, C.; Tse-Sheepy, I.; Dickson, J. *J. Appl. Polym. Sci.* **1997**, *65*, 109–116.
- (13) Yang, J.; Wang, M.; Hsu, Y.; Chang, C. *J. Appl. Polym. Sci.* **1997**, *65*, 109–116.
- (14) Trushinski, B.; Dickson, J.; Childs, R.; McCarry, B. *J. Appl. Polym. Sci.* **1993**, *48*, 187–198.
- (15) Trushinski, B.; Dickson, J.; Childs, R.; McCarry, B.; Gagnon, D. *J. Appl. Polym. Sci.* **1994**, *54*, 1233–1242.
- (16) Ji, J.; Trushinski, B.; Childs, R.; Dickson, J.; McCarry, B. *J. Appl. Polym. Sci.* **1997**, *64*, 2381–2398.
- (17) Ulbricht, M. *React. Funct. Polym.* **1996**, *31*, 165–177.
- (18) Lee, Y. M.; Ihm, S.; Shim, J.; Kim, J.; Cho, C.; Sung, Y. *Polymer* **1995**, *36*, 81–85.
- (19) Mika, A.; Childs, R.; Dickson, J.; McCarry, B.; Gagnon, D. *J. Membr. Sci.* **1995**, *108*, 37–56.
- (20) Mika, A.; Childs, R.; Dickson, J.; McCarry, B.; Gagnon, D. *J. Membr. Sci.* **1997**, *135*, 81–92.

been focused on decreasing fouling during the filtration of biological solutions.

The work reported here is part of a larger effort to modify membranes that exhibit low protein adhesion and lower fouling using UV-assisted graft polymerization.^{3,4,21–27} Two photograft methods, dip and immersion,²³ and two similar polymers, polysulfone and poly(ether sulfone),^{21,22,24} have been recently compared. Because the polysulfones are UV-active, and do not require an initiating agent for photooxidation, they have been the focus of our research. Pieracci et al.²⁵ have increased the selectivity of the UV-irradiation by replacing 254-nm wavelength lamps with less energetic 300-nm wavelength lamps with short wavelength filters (<280 nm)²⁵ and without such filters.²⁶ Optical filters were not used here. We have also described the mechanism of bulk polymer chain scission (cleavage) and radical formation during photooxidation of poly(aryl sulfones).³ The choice of monomer has been recently evaluated in some depth.²⁷

Three critical aspects of graft-induced polymerization of poly(ether sulfone) membranes for optimizing ultrafiltration performance with protein solutions are addressed here. They include modification conditions (monomer type and concentration, and energy of irradiation with 300-nm lamps), choice of membrane structure (skin thickness), and an evaluation of the washing conditions after modification (with ethanol or water). The objective of this study was to evaluate how various operating parameters of UV-assisted graft polymerization of *N*-vinyl-2-pyrrolidinone on commercial asymmetric (skinned) PES membranes (total thickness ~250 μm ; skin thickness ~2–10 μm) in the dip-mode of operation effect filtration performance. Each modified membrane was characterized via several parameters, including attenuated total reflection infrared spectroscopy (ATR-IR) to evaluate the degree of grafting (DG), atomic force microscopy (AFM) to obtain a measure of the surface roughness, scanning electron microscopy (SEM) to observe the membrane architecture and structure, and ultrafiltration (UF) to determine the change in performance with UV-assisted graft polymerization parameters.

After presenting the experimental materials and methods, we summarize the transport equations in the Theoretical Section. Then, in the Results and Discussion section, we show how the amount grafted depends on the washing solution (ethanol or water), the molecular weight cutoff (MWCO) of the membrane, and the percentage monomer in the solution. Using an AFM and a simple 2-dimensional zigzag model of the surface, we

report the effects of surface modification parameters (irradiation time and monomer concentration) and membrane porosity (MWCO) on change in the surface roughness. Next, filtration performance characteristics (resistance and BSA rejection) are measured and correlated with modification parameters, membrane porosity, and cleaning solution type. This work provides a prescription on how to produce a modified PES membrane with low fouling properties while maintaining filtration performance.

Experimental Section

Materials. The poly(ether sulfone) (PES) base membranes had 50, 70, and 100 kDa MWCO (OMEGA series, lots 9140E, 7309A, and 7265G, respectively, from Pall Filtron Corp., East Hills, NY). These base membranes were slightly hydrophilized by the manufacturer by an undisclosed process. These membranes were used for modification and analysis as received. *N*-vinyl-2-pyrrolidinone (NVP; Aldrich, Milwaukee, WI) was chosen as the monomer for the UV-initiated graft-polymerization, and was vacuum distilled to remove the inhibitor before use. Ultrahigh-purity nitrogen gas (Matheson, Secaucus, NJ) was used during the dip modification process. Deionized water was produced from tap water using an in-house deionized water system consisting of (in order) reverse osmosis membranes (FT-30, FilmTech, MN), UV irradiation, and a Teflon microfilter. The PES membranes were dipped in deionized water overnight and washed several times with deionized water before use in order to remove surfactant. Nitrogen gas (Matheson, Secaucus, NJ) was of ultrahigh purity.

Preparation of Modified Membranes. The 50, 70, and 100 kDa membranes were modified using UV-induced graft polymerization. A Rayonet photochemical chamber reactor system (model RPR-100, Southern New England Ultraviolet Co., Branford, CT) contained 300-nm UV lamps (~15% of the energy was below 280 nm). The same UV reactor was used previously with 254-nm UV lamps^{22,23} and with the dip modification technique.^{23–27} In this method, membranes were dipped in NVP monomer solution for 30 min with stirring at 22 °C, removed from the monomer solution, N_2 purged for 10 min, and irradiated in water-saturated N_2 for a specified time. After modification, the membranes were washed with deionized water in a shaker for 2 h. The modification scheme is similar to that of Pieracci et al.²³ In this study, ethanol washing meant dipping in ethanol for 24 h before use.

Degree of Grafting. As with the previous research,^{22–27} attenuated total reflection Fourier transform infrared spectroscopy (ATR/IR) (Magna-IR 550 Series II, Nicolet Instruments, Madison, WI) was used to obtain a measure of the DG. Using an incident angle of 45°, the penetration on sample depth was approximately 0.1–1.0 μm .²⁸ The DG was defined as the ratio of the absorbance peak height at 1678 cm^{-1} of the amide I carbonyl group of the five-membered ring of the NVP molecule to that at 1487 cm^{-1} of the benzene carbon–carbon double bond. Because NVP is highly water soluble, it is not easy to completely remove the influence of the water peak at 1678 cm^{-1} . Therefore, in this study, the DG that was previously used was modified by accounting for the water (OH stretching) peak at 3440 cm^{-1} , i.e.

$$\text{DG}_{\text{mod}} = \text{DG}_{\text{mes}} - H_{3440}/H_{1487} \times 0.177 \quad (1)$$

where DG_{mes} was the measured DG, and H_{3440} and H_{1487} were the height of the peaks at 3440 and 1487 cm^{-1} , respectively. The 0.177 is the ratio of the water peak at 1678 cm^{-1} to the water peak at 3440 cm^{-1} , which was obtained from the actual peak measurement for the same modified membranes with different contents of water. $H_{3440}/H_{1487} \times 0.177$ accounts for the influence of water on the peak at 1678 cm^{-1} .

(21) Crivello, J. V.; Yamagishi, H.; Belfort, G. Low fouling ultrafiltration and microfiltration aryl polysulfone. U.S. Patent Number 5,468,390; 1995.

(22) Pieracci, J.; Crivello, J. V.; Belfort, G. *J. Membr. Sci.* **1999**, *156*, 223–240.

(23) Pieracci, J.; Wood, D. W.; Crivello, J. V.; Belfort, G. *Chem. Mater.* **2000**, *12*, 2123–2133.

(24) Kaeselev, B.; Pieracci, J.; Belfort, G. *J. Membr. Sci.* **2001**, *194*, 245–261.

(25) Pieracci, J.; Crivello, J. V.; Belfort, G. *Chem. Mater.* **2002**, *14*, 256–265.

(26) Pieracci, J.; Crivello, J. V.; Belfort, G. *I. J. Membr. Sci.* **2002**, *202*, 1–16.

(27) Taniguchi, M.; Belfort, G. Low protein fouling synthetic membranes by UV-assisted graft polymerization: Varying monomer type. Submitted for publication.

(28) Contact Sampler User's Manual for Model 0012-490(T) Nicolet Magna-IR; Nicolet Instruments: Madison, WI.

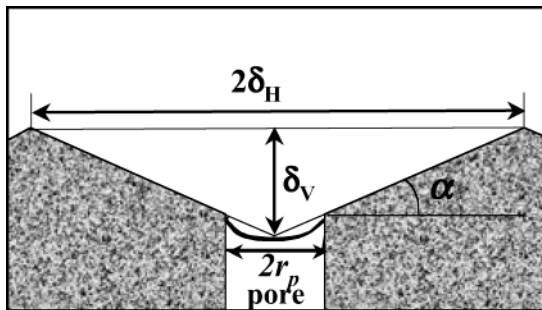


Figure 1. Model zigzag cross-section of a membrane surface and definitions of the mean horizontal, δ_H , and vertical, δ_V , length scales, obtained from >300 AFM roughness measurements.

Energy Absorbance Measurements. The amount of emitted energy from the UV lamps that reached the membrane surface during modification was measured using a compact radiometer (UV Process Supply, Inc., Chicago, IL). A quartz vessel was filled with air, and the whole assembly was placed in the center of the UV reactor such that the total path length was 9 cm. The quartz vessel was designed with a path length of 1 cm, which was the distance between the membrane and the wall of the quartz reactor. Measurements were taken in duplicate. Full wavelength scans of various solutions were performed using a double-beam UV/VIS spectrophotometer (U 2000, Hitachi Instruments, Inc., Danbury, CT).

Surface Structure (Roughness) and Skin Thickness. Topographical images of $5 \times 5 \mu\text{m}^2$ sections of membrane surfaces were made in contact mode using SiN₂ cantilevers (Park Scientific Instruments, Sunnyvale, CA) with an atomic force microscope (AFM, Auto Probe PC, Park Scientific Instruments) and surface analysis and data acquisition software (Pro Scan ver 1.5, Park Scientific Instruments). Mean horizontal, δ_H , and a vertical, δ_V , length scales, which are shown in Figure 1, were obtained from more than 300 measurements of the depth (mean vertical distance of top of peak to bottom of trough) and the width (mean horizontal peak to peak) for each membrane, respectively. Additional details are available from Taniguchi et al.^{29,30} A scanning electron microscope (SEM, ETEC Autoscan, ETEC Corporation, Hayward, CA) was used for the skin thickness determination.

Filtration. Filtration System. A dead-end stirred cell filtration system was designed to characterize the filtration performance of unmodified and modified membranes.²² The system consisted of a filtration test cell (model 8010, Millipore Corp., Bedford, MA) whose total inner volume was 18.5 mL, and a 1-L reservoir. The membrane area was 3.8 cm^2 . The feed side of the system was pressurized by extra-dry grade nitrogen. All filtration experiments were conducted at a constant transmembrane pressure at 69 kPa (10 psig), a stirring rate of 500 rpm, and a system temperature of $22 \pm 1^\circ\text{C}$. Additional details are given by Pieracci et al.²³

Bovine Serum Albumin (BSA) Solutions. Bovine serum albumin (BSA, essentially fatty acid free, $>98\%$, lot 48H1028) was obtained from Sigma Chemical Co. (St. Louis, MO). BSA (1.0 g) in 1 L of 10 mM phosphate buffered saline (PBS) at pH 7.4 was used for the feed solution. The isoelectric point of BSA is 4.7, and it has a charge of approximately -20.5 electrons at pH 7.4.³¹ Both the buffer and protein solution were pre-filtered through a $0.22\text{-}\mu\text{m}$ nylon membrane prior to use. Protein concentrations were determined spectrophotically at 280 nm using a Hitachi U 2000 double-beam UV/VIS spectrophotometer (Hitachi Instruments, Inc., Danbury, CT) and used to prepare a calibration curve.

(29) Taniguchi, M.; Pieracci, J.; Belfort, G. *Langmuir* **2001**, *17*, 4312–4315.

(30) Taniguchi, M.; Belfort, G. *Langmuir* **2001**, *18*, 6465–6467.

(31) Creighton, T. *Proteins: Structures and Molecular Properties*; Freeman and Company: New York, 1984.

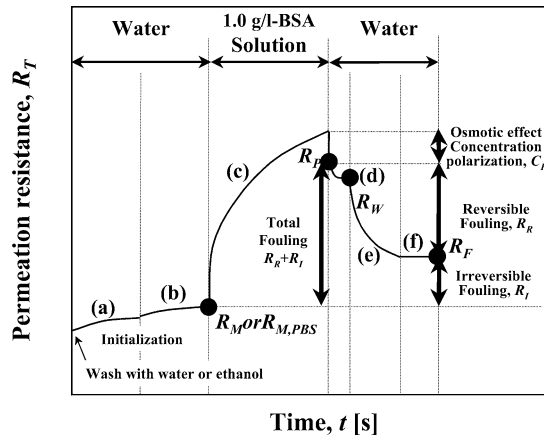


Figure 2. BSA filtration protocol: (a) to minimize compaction effects deionized water was passed through the membrane at the transmembrane pressure of 172 kPa (25 psig) for 15 min; (b) the measured stable water permeation resistance at 69 kPa (10 psig) (R_M); (c) after the cell was emptied, 1 g of BSA per L of solution was filled and the 69 kPa (10 psig) was reapplied, and the filtration was continued until 20 mL of permeate was collected with continual addition of BSA solution to the cell during filtration. (d) The cell was then emptied and refilled with deionized water and the water permeation resistance (R_W) was measured with stirring; (e) the membrane was oriented in the reverse direction in the cell and deionized water was passed at a pressure of 172 kPa (25 psig), (f) the membrane was repositioned to its original orientation and the water permeability was again measured (R_F). All filtration steps were operated at $22 \pm 1^\circ\text{C}$.

Filtration Protocol. A schematic representation of the filtration protocol is shown in Figure 2. Each membrane was first compacted for 15 min at 172 kPa (25 psig). The pressure was lowered to the operating pressure of 69 kPa (10 psig). The water or PBS permeation resistance (R_M , or $R_{M,PBS}$ [$\text{m}^2 \cdot \text{Pa} \cdot \text{s} / \text{kg}$]) was measured at different times for the every gram of permeate collected until it was relatively constant ($<2\%$ change in R_M). Then the cell was filled with the BSA solution from the reservoir and re-pressurized. The flux and permeate concentration were then measured for each gram of permeate. After 20 g of permeate were collected, the BSA concentration in the cell was measured and the time course change of BSA solution in the cell was calculated from a mass balance. BSA rejection for each gram of permeate was obtained from the concentration of feed and permeate. The cell was then emptied and refilled with water and the water permeation resistance (R_W) after BSA filtration was measured. The membrane was then oriented in the reverse direction in the cell and back-washed with water at a pressure of 172 kPa (25 psig) for the time required for 20 g of permeate to pass through pores as calculated from R_W . The membrane was then repositioned to its original orientation and the water permeability (R_F) was again measured. The measurement error for the permeability was $\pm 2.5\%$. To account for temperature variations, the permeation resistance was normalized to the values at 25°C as $R_{25} = R_T \cdot \eta_{25} / \eta_T$, based on the water viscosity at 25°C (η_{25} , $\text{N} \cdot \text{s} / \text{m}^2$) and at the operating temperature, $T^\circ\text{C}$ (η_T , $\text{N} \cdot \text{s} / \text{m}^2$).

Theory

The hydrodynamic resistance of water permeation (no salts or protein) for a new membrane is calculated from

$$R_M = \frac{\Delta P}{J_{V0}} \quad (2)$$

Initially, the solution permeation (with salts and protein) is given by

$$J_{VP,0} = \frac{\Delta P - \sigma \cdot \Delta \pi(C_W)}{R_M} \quad (3)$$

and at the end of the run, it is given by

$$J_{VP,P} = \frac{\Delta P - \sigma \cdot \Delta \pi(C_W)}{R_P} \quad (4)$$

Here, $J_{VP,0}$ is the initial solution flux [$\text{kg}/\text{m}^2 \cdot \text{s}$], $J_{VP,P}$ is the final solution flux [$\text{kg}/\text{m}^2 \cdot \text{s}$], ΔP is the trans-membrane pressure, $\Delta \pi(C_W)$ is the osmotic pressure at the membrane wall concentration (C_W) and was measured by Vilker et al.³² The symbol σ is a reflection coefficient, which is approximately equal to the maximum solute rejection obtained at high ΔP . BSA rejection was used to approximate σ , because BSA rejection did not change under the experimental conditions of this study.

The concentration polarization effect can be expressed using the film boundary layer theory³³ as

$$\frac{C_W - C_P}{C_B - C_P} = \exp\left(\frac{J_{VP,0}}{k}\right) \quad (5)$$

where C_B is the bulk concentration of feed, C_P is the permeate concentration, and k is the mass transfer coefficient. Maximum value for C_W and k for BSA in our filtration system were obtained with almost 100% BSA rejection ($C_P \approx 0$) by measuring various $J_{VP,0}$ values. For this condition, eq 5 can be expressed as

$$J_{VP,0} = -k[\ln(C_B) - \ln(C_W)] \quad (6)$$

And $k = (7.30 \pm 0.09) \times 10^{-6}$ [m^2/s] was obtained from the slope of a plot of $J_{VP,0}$ ($\times 10^{-6}$ $\text{m}^3/\text{m}^2 \cdot \text{s}$) versus $\ln(C_W)$ where C_B is in g/L and $y = 7.3033 \ln(x) + 38.676$; $R^2 = 0.958$. The maximum $C_W = 199 \pm 14$ [g/L], was obtained from the x intercept. They are reasonable values compared with those reported by others.³⁴

Results and Discussion

Membrane Polymer Scission and Formation of Homopolymer. Using UV irradiation to activate the surface of PES (produce radical sites) for grafting of vinyl monomers and their subsequent polymerization has been successfully used to change the surface characteristics and hence the performance of PES ultrafiltration membranes.^{22–27} PES has also been shown to be more sensitive than poly(sulfone) to UV irradiation.²⁴ Because of this sensitivity to UV, bulk polymer chain scission (cleavage) and multiple radical sites are easily obtained. The problem, however, is that abundance of such cleavage negatively effects the membrane pore structure, often resulting in increased permeation flow rate and decreased solute retention.^{22,23} Pieracci et al.²⁵ have reduced these unwanted effects by selecting longer

(32) Vilker, V. L.; Colton, C. K.; Smith, K. A. *J. Colloid Interface Sci.* **1981**, *79*, 548.

(33) Blatt, W. F.; Dravid, A.; Michaels, A. S.; Nelson, L. Solute polarization and cake formation in membrane ultrafiltration: causes, consequences, and control techniques. In *Membrane Science and Technology*; Flinn, J. E., Ed.; Plenum Press: New York, 1970.

(34) Opong, W. S.; Zydny, A. L. *AIChE J.* **1991**, *37*, 1497–1510.

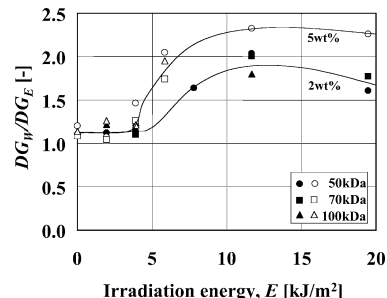


Figure 3. Comparison of degrees of grafting of the membranes after washing in ethanol (DG_E) and in water (DG_W) expressed as the ratio of DG_W/DG_E versus irradiation energy, E : (●) 50 kDa with 2 wt % NVP; (■) 70 kDa with 2 wt % NVP; (▲) 100 kDa with 2 wt % NVP; (○) 50 kDa with 5 wt % NVP; (□) 70 kDa with 5 wt % NVP; and (△) 100 kDa with 2 wt % NVP.

wavelength UV such as 300 nm as opposed to the 254 nm used earlier. We chose the same approach here.

Although graft-polymerization is desired over homopolymerization in the pores, it is difficult to distinguish between these phenomena using only DG as a measure of graft amount. Previously,^{21–24} after modification, the PES membranes were washed with water to attempt to remove entrapped nongrafted water-soluble NVP and other fragments from the pore surface. To further test for the presence of homopolymer, the relative amount of graft-induced polymerization for 2 and 5 wt % NVP and with three UF PES membranes (50, 70, and 100 kDa) was measured in separate experiments after 24 h of washing the membranes in water and ethanol. The results are presented in terms of degree of grafting after post-washing in ethanol (DG_E) and in water (DG_W). A plot of the ratio of (DG_W/DG_E) versus amount of exposed irradiation energy (E) [kJ/m^2] is shown in Figure 3 for both NVP concentrations and all three UF membranes. For $E < 4 \text{ kJ}/\text{m}^2$, very little homopolymer formation was observed (i.e., $DG_W/DG_E \approx 1.2$ and constant) suggesting that just sufficient irradiation energy was used resulting in effective grafting but negligible bond cleavage. The as-received membranes exhibited a small peak at 1678 cm^{-1} suggesting that the membranes came with an additive (possibly NVP). Washing with ethanol was likely able to remove the additives more effectively than water explaining the $(DG_W/DG_E) > 1.0$ at zero irradiation.

For $E > 4 \text{ kJ}/\text{m}^2$, (DG_W/DG_E) increased rapidly reaching saturation at $E \approx 12 \text{ kJ}/\text{m}^2$ with ratio values of 1.8 and 2.3 for 2 and 5 wt % NVP solutions, respectively. To further understand the photoinduced graft polymerization process and its effects, and the morphology and permeability of the PES membranes, the water permeation resistance (under stable conditions) was measured before and after immersing 50 kDa unmodified and modified (2 wt % NVP, $E = 7.8 \text{ kJ}/\text{m}^2$) PES UF membranes into different concentrations of ethanol for 24 h. The modified membranes showed a greater decrease in water permeation resistance, R_M , than the unmodified membranes (Figure 4). This suggests that increasing amounts of ethanol were able to remove increasing amounts of entrapped homo-polymer and other nonpermanently grafted (additives) material from the pores. Also, the difference between R_M for the unwashed and the ethanol-washed membranes was

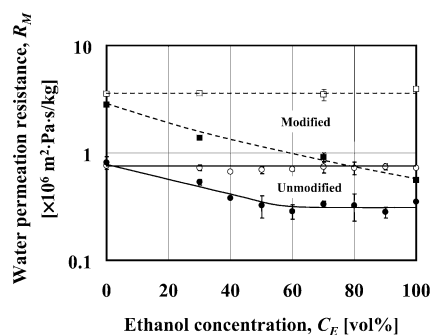


Figure 4. Change in water permeation resistance after washing in ethanol for 24 h: (○) unmodified 50 kDa after washing in water (before washing in ethanol); (●) unmodified 50 kDa after washing in ethanol; (□) modified (2 wt % NVP, $E = 7.8 \text{ kJ/m}^2$) 50 kDa before washing in ethanol; (■) modified 50 kDa after washing in ethanol.

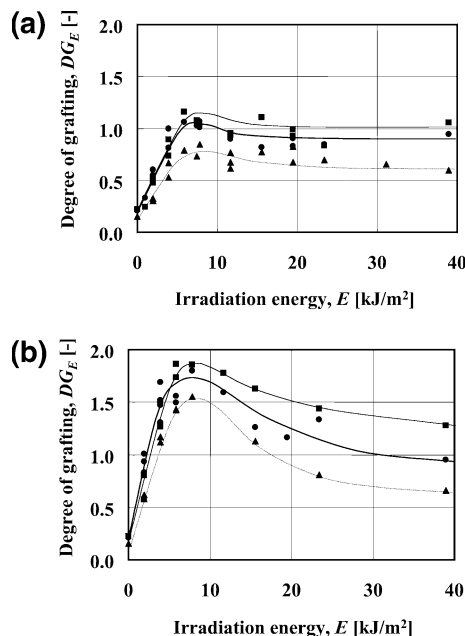


Figure 5. Effect of irradiation energy on the degree of grafting after washing in ethanol for (a) 2 wt % NVP and (b) 5 wt % NVP. The MWCO values were (●) 50 kDa; (■) 70 kDa; and (▲) 100 kDa.

greater for the modified membranes than for the unmodified membranes. Clearly, more entrapped material was formed (and hence removed by ethanol) from the former than the latter membranes. Above 60% ethanol concentration, little change was observed for R_M for the unmodified membrane suggesting all the entrapped material was removed and further increases in ethanol concentration were ineffective. From an industrial and FDA viewpoint, such ethanol washing would be required to prevent slow efflux of additives.

Grafting Polymerization. The relationship between degree of grafting measured by ATR/FTIR and irradiation energy is shown in Figure 5, in which the membranes were immersed in 2 and 5 wt % of NVP solutions prior to irradiation. All curves indicate that the grafting grew linearly at low irradiation energies ($< 4-5 \text{ kJ/m}^2$). This suggests that effective cleavage and grafting occurred. At larger irradiation energies ($\sim 5-8 \text{ kJ/m}^2$), DG reached a maximum for all concentrations and energies. Figure 6 displays linear dependence of net DG on the product of the monomer concentration (C_{NVP}) and ir-

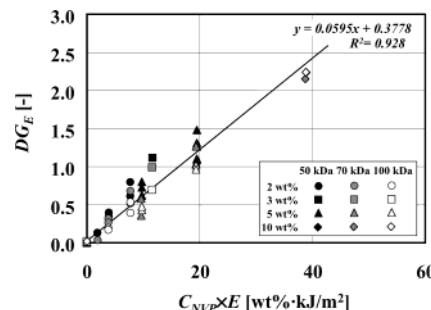
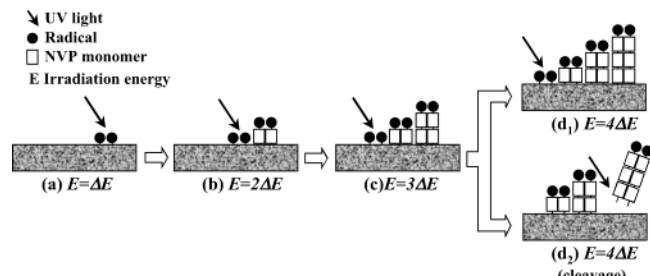


Figure 6. Relationship between degree of grafting (DG_E) versus NVP concentration (C_{NVP}) times irradiation energy (E) for $E < 4 \text{ kJ/m}^2$: (●) 50 kDa with 2 wt % NVP; (■) 50 kDa with 3 wt % NVP; (▲) 50 kDa with 5 wt % NVP; (◆) 50 kDa with 10 wt % NVP; (●) 50 kDa with 2 wt % NVP; (■) 50 kDa with 3 wt % NVP; (▲) 50 kDa with 5 wt % NVP; (◆) 50 kDa with 10 wt % NVP; (○) 100 kDa with 2 wt % NVP; (□) 100 kDa with 3 wt % NVP; (△) 100 kDa with 5 wt % NVP; and (◇) 100 kDa with 10 wt % NVP.

Scheme 1



radiation energy (E) up to 4 kJ/m^2 for three different MWCO PES UF membranes and four different monomer concentrations. This correlation appears to be independent of MWCO of the membrane and has a correlation coefficient value of $R^2 = 0.93$. The slope was $5.95 \times 10^{-2} \text{ m}^2/\text{kJ} \cdot \text{wt} \%$. A schematic of a proposed photoreaction process for $E < 4$ is shown in Scheme 1. Here, the number of radical sites formed increases proportionally with irradiation energy because there is no obstacle for UV light to reach the membrane in the dip modification method. This simply suggests that the relationship between the degree of grafting (DG) and the irradiation energy (E) should be linear at low irradiation energy and that DG should also be proportional to the monomer concentration. Similar behavior was also observed in previous work,²³ in which a different modification technique (immersion method) was used. In summary, these results support the explanation that chain scission and effective grafting occur at $E < 4 \text{ kJ/m}^2$ (Figure 3) but that at $E \geq 4 \text{ kJ/m}^2$, substantial homopolymerization occurs reducing DG (Figure 5).

Irradiation, Surface Roughness, and Morphology. Because surface roughness is thought to influence platelet adhesion during membrane dialysis,³⁵ it is important for protein adhesion studies to determine the influence of UV-irradiation with and without graft polymerization on surface roughness, and the extent of that influence. An added benefit would be to know how membrane morphology (i.e., top dense layer or skin thickness) is relevant. Two roughness parameters, δ_V

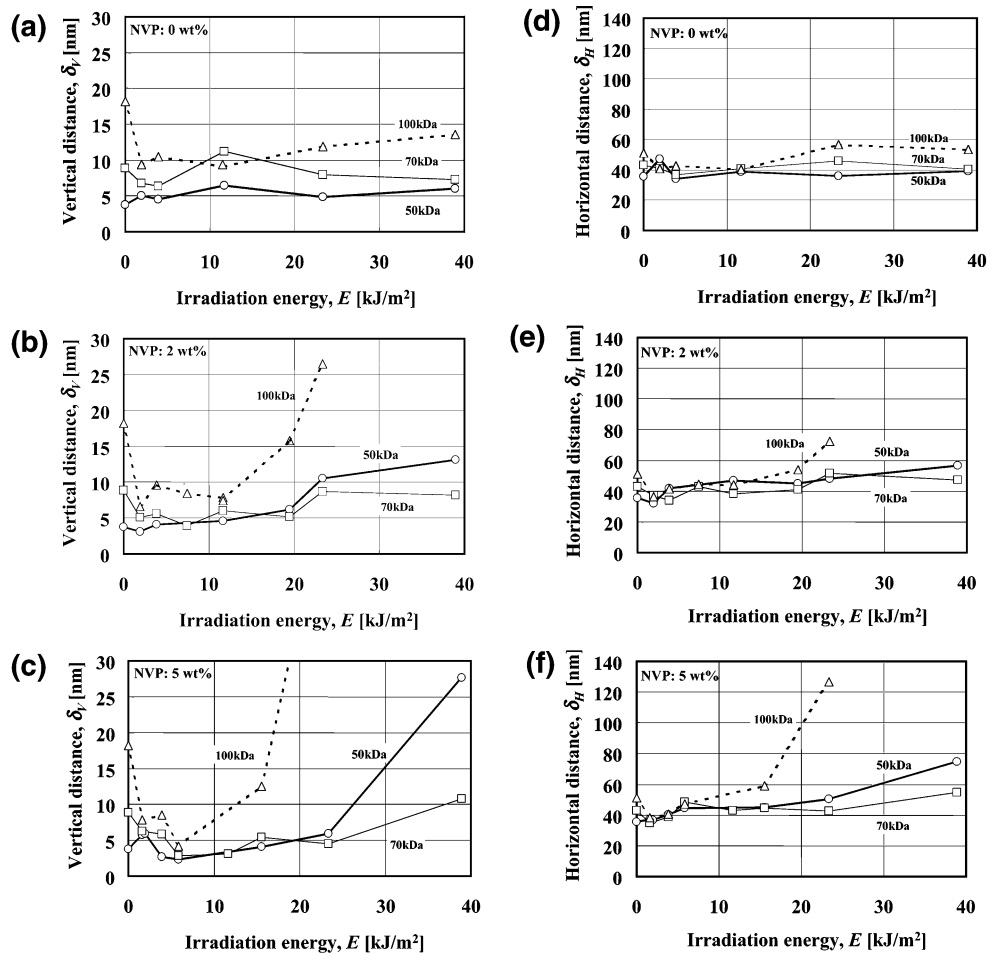


Figure 7. Vertical (δ_V) (a–c) and horizontal (δ_H) (d–f) distances analyzed from the topography of the membrane surface and measured by AFM. Vertical distance versus E for (a) water, (b) 2 wt % NVP, and (c) 5 wt % NVP. Horizontal distance versus E for (d) water, (e) 2 wt % NVP, and (f) 5 wt % NVP for (○) 50 kDa; (□) 70 kDa; and (△) 100 kDa PES UF membranes.

and δ_H , (Figure 1) from AFM measurements and the skin thickness results from SEM measurements were used.

The change in vertical (δ_V) and horizontal (δ_H) distance with MWCO of PES unmodified (pre-irradiation) and modified (with irradiation) membranes for 0, 2, and 5 wt % NVP were followed as a function of irradiation energy E (Figure 7). First, irradiation E had a noticeable effect on roughness (δ_V and δ_H) with or without pre-immersion in NVP solution. Second, to a greater or lesser extent, the curves are mostly strongly or weakly concave upward with a minimum roughness region at low E values of 2–12 kJ/m². Third, the order of sensitivity of the roughness parameters to E appears to be directly related to the membrane skin thickness, δ_S (3, 8, and 2 μ m for the 50, 70, and 100 kDa MWCO, respectively) (Figure 8). Thus, at higher values of E (>10 –12 kJ/m²), δ_V and δ_H increased more strongly for the 100 > 50 > 70 kDa MWCO membranes, where skin thickness also follows this order. Clearly, at low E values, photoinduced grafting dominates and the surfaces become smoother, whereas at high E values, homopolymerization, chain scission, and surface etching become important as the monomer concentration is depleted. The minima discussed above for Figure 7 correlated with the maxima observed in Figure 5 and occur in a similar range of E , giving consistency to the results.

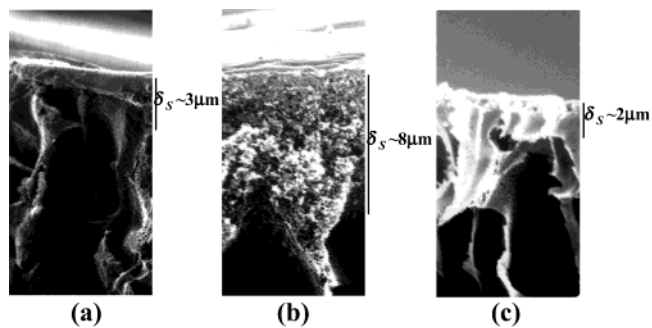


Figure 8. Scanning electron micrographs of the three membrane surface (skin layer) cross-sections. The MWCOs of the PES UF membranes were (a) 50 kDa, (b) 70 kDa, and (c) 100 kDa. Estimates of the mean skin thickness were 3, 8, and 2 μ m, for the 50, 70, and 100 kDa MWCO membranes, respectively.

Ultrafiltration (UF). The effect of post-modification (2 wt % NVP) washing with ethanol or water for 24 h on UF performance is shown in Figure 9. The effect of washing with ethanol (Figure 9a, b, and c) was quite different from that of washing with water (Figure 9d, e, and f). First, R_M increased slightly and dramatically with increasing E for ethanol and water, respectively, for $E < 8$ kJ/m² (Figure 9a and d). Second, removal of homopolymer and other photoproduced fragments with ethanol washing resulted in a fast drop in R_{BSA} with increasing E (Figure 9b). Absent this removal (with

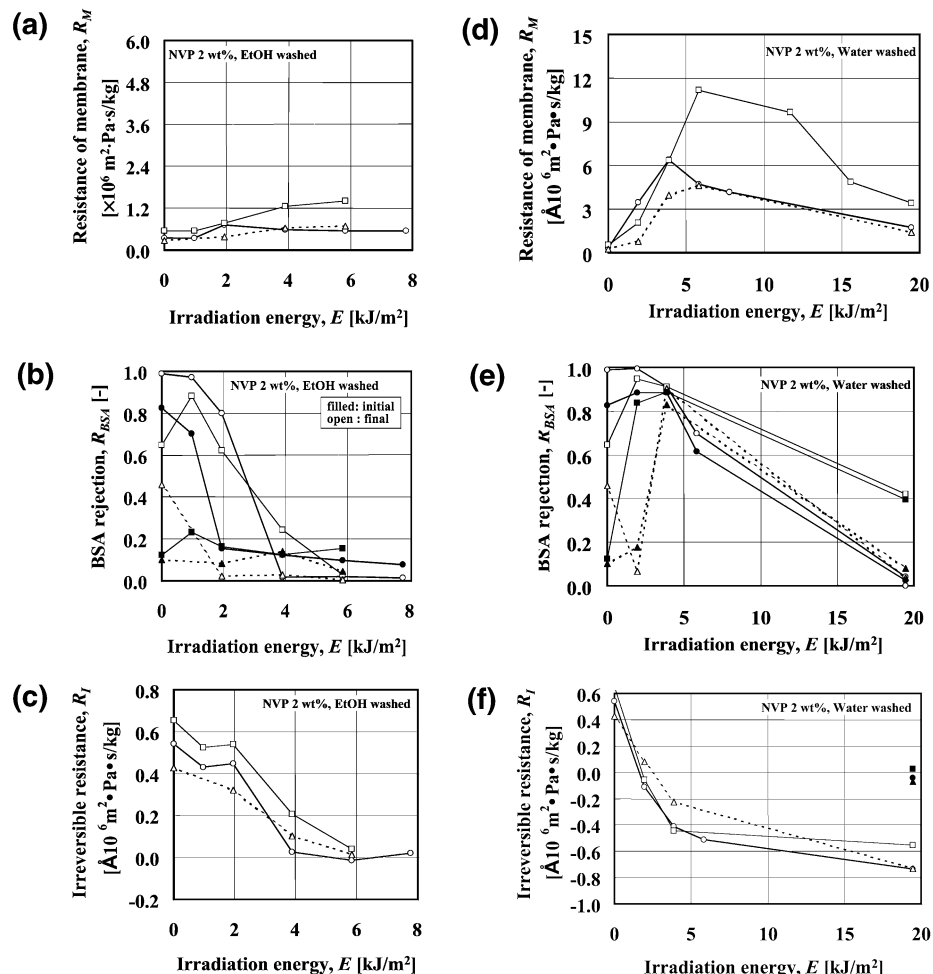


Figure 9. Filtration properties of membranes modified with 2 wt % NVP after modification and washing with ethanol (a–c) or water (d–f) as a function of irradiation energy: (a, d) resistance of membranes, R_M ; (b, e) BSA rejection, R_{BSA} ; and (c, f) irreversible fouling, $R_I = R_F - R_M$; (●, ○) 50 kDa; (■, □) 70 kDa; (▲, △) 100 kDa.

water washing), R_{BSA} remained higher at larger E (Figure 9e). Third, increasing photograft polymerization with increasing E improved the wettability of the surfaces and reduced $R_I (= R_F - R_M)$ and hence fouling (Figure 9c and f). During the UF experiment, R_{BSA} increases and decreases from the start (initial) to the end (final) of the run for low ($E < 2 \text{ kJ/m}^2$) and high ($E > 2 \text{ kJ/m}^2$) E values, respectively. Thus, during photografting at low E , BSA monomers, dimers, and trimers can adsorb or be trapped in the pores and effect an increase in R_{BSA} . At higher values of E , when chain scission dominates, the resulting homopolymer fragments could easily be entrapped and decrease the mean pore size (pore plugging), resulting in higher R_{BSA} temporarily during the start of the run. Later these fragments could be washed out, allowing R_{BSA} to drop. The drop in R_I was substantial and less so for ethanol and water washes, respectively, for all three membranes with increasing E (Figure 9c and f). The difference, however, between ethanol and water washing is that for the latter case R_I becomes negative, i.e., the modified membranes were more permeable than the original membrane. A duplicate run gave R_I values close to zero (filled symbols in Figure 9f). The adsorbed BSA plugging the pores and the presence of irradiation fragments may have passed through the membranes for protein solutions (break-through) as previously noted by Koehler et al.³⁶

A series of experiments similar to those presented in Figure 9 for 2 wt % NVP, was conducted for 5 wt % NVP with post-washing with ethanol or water. The results with the higher concentration of NVP (not shown) showed trends similar to those seen with the 2 wt % NVP. However, at the higher NVP concentration higher DG (Figure 5) and higher values of R_{BSA} were observed. Also, R_I decreased to zero at $C_{NVP} = 5 \text{ wt } \%$ and $E = 4 \text{ kJ/m}^2$ for the ethanol washed cases.

Conclusions

With the increasing realization by membrane manufacturers that surface modification of synthetic polymeric membranes is economically and technically attractive, understanding the underlying mechanisms of the modification process has become important. The work reported here focused on three critical aspects of graft-induced polymerization of poly(ether sulfone) membranes for optimizing ultrafiltration performance with protein solutions are addressed here. They include modification conditions (monomer type and concentration, and energy of irradiation with 300-nm lamps), choice of membrane structure (skin thickness), and evaluation of the washing conditions after modification

(with ethanol or water). Using a commercially attractive dip-method, with UV-sensitive PES UF membranes of 50, 70, and 100 kDa MWCOs, we grafted 2–10 wt % NVP using our standard photooxidation protocol with 300-nm lamps. Specific conclusions are summarized as follows. (1) Homopolymerization and main-chain scission without grafting, two undesired phenomena, can be minimized by operating below a critical irradiation energy, $E < 4 \text{ kJ/m}^2$ and with up to 5 wt % NVP monomer concentration for all three UF membranes. (2) A universal linear plot between net amount grafted DG_E and the product of the NVP concentration, C_{NVP} and the irradiation energy, E , for $E < 4 \text{ kJ/m}^2$ was obtained with an excellent correlation coefficient of $R^2 = 0.93$ for four NVP concentrations (0, 2, 3, and 5) and three UF membranes (50, 70, and 100 kDa). (3) There appears to be a relationship between the thickness of the dense or skin layer and the membrane surface roughness (as measured by δ_V and δ_H from AFM estimates) resulting from surface modification. This is a qualitative conclusion as more data are needed for added confidence. For $E < 4 \text{ kJ/m}^2$ both δ_H and δ_V decreased with increasing E , while the reverse trends were seen for $E > 4 \text{ kJ/m}^2$ for all three membranes. (4) Washing with ethanol or water after completion of the UV-assisted graft polymerization of PES has distinctly different effects. Ethanol was able to effectively remove entrapped homopolymer and other fragments resulting from chain-scission without grafting. Water was less proficient. (5) UV-assisted graft polymerization of NVP on PES UF membranes can effect a substantial reduction in irreversible membrane fouling.

In general, as a result of this and previous work, we can now suggest a protocol for optimizing graft-assisted photopolymerization of PES UF membranes. Once a monomer has been chosen (see ref 27 for direction; this will depend on the functionality for which one wants to cover the surface), the modification conditions can be specified using 300-nm lamps by preparing a universal correlation similar to that shown in Figure 6 for the chosen monomer. Then, keeping the DG value ~ 0.2 –1.0 according to past experience (higher values usually result in a significant and unacceptable drop in permeation rates), the wt % and irradiation energy, $E < 4$ (to minimize homopolymer formation, Figure 5), can be chosen. Next, a suitable PES membrane is chosen on the basis of the desired molecular weight cutoff. If increased roughness is desired, then relatively thin skin layers would be appropriate (Figures 7 and 8). Post-modification washing with ethanol will stabilize the membrane performance in terms of water permeability and protein retention, and impart long-term high performance with minimal irreversible fouling (Figure 9).

Acknowledgment. We thank Pall Filtron Corporation for supplying the PES membranes. We appreciate the assistance of Dr. Thomas Baekmark for his help with AFM measurements. We also acknowledge the support of Toray Industries Inc., Shiga, Japan, and grants to Georges Belfort by the U.S. Department of Energy (grant DE-FG02-90ER14114) and the National Science Foundation (grant CTS-94-00610).

CM020283P